Osmotic pressure, light scattering and counterion condensation in polyelectrolyte solutions

Elmira Abbasi Garehtapeh,[1] Anish Gulati,[2] Takaichi Watanabe,[3] and Carlos G. Lopez[4]
[1)]*Materials Science and Engineering departments, The Pennsylvania State University, 1 Pollock Rd, State College, 16802, US*
[2)]*Institute of Physical Chemistry, RWTH Aachen University, Landoltweg 2, 52056 Aachen, Germany, European Union*
[3)]*Department of Applied Chemistry, Graduate School of Natural Science, Okayama University, 3-1-1, Tsushima-naka, Kita-ku, Okayama 700-8530, Japan*
[4)]*Materials Science and Engineering departments, The Pennsylvania State University, 1 Pollock Rd, State College, 16801, US*

(*Electronic mail: cvg5719@psu.edu)

The scattering behaviour of polyelectrolytes is a long-standing puzzle: based on their high osmotic pressure, polyelectrolytes should be incompressible systems in which long-ranged concentration fluctuations are strongly suppressed, meaning that their low-q scattering should be extremely weak. In contrast to this, small angle scattering experiments consistently report a 'low-q upturn' which results in a zero-angle scattering intensity several orders of magnitude larger than the theoretically predicted one. Here we show that the low-q upturn, and the corresponding slow mode can be largely removed by filtration. Any remaining contribution can be subtracted by using dynamic light scattering to split the total scattering signal of a polyelectrolyte solution into fast and slow components. This static intensity of the fast component corresponds to the osmotic compressibility of the system calculated from osmotic pressure measurements and can be used to determine the fraction of free counterions in aqueous and non-aqueous solvents, as demonstrated for carboxymethyl cellulose in water, sodium polyglutamate in water and ethylene glycol and magnesium polyglutamate in water. Our results demonstrate a light scattering method to quantify the osmotic pressure of salt-free polyelectrolyte solutions in non-aqueous media, which is difficult using conventional osmometric techniques.

I. INTRODUCTION

When a polyelectrolyte dissolves in a solvent, a fraction of its counterions are released into the solvent bulk.[1–4] These are known as free counterions, and they are responsible for the huge osmotic pressure (Π) of polyelectrolyte solutions. Specifically, the scaling theory[5–7] expects:

$$\Pi/k_BT \simeq fc + \frac{1}{\xi^3} \qquad (1)$$

where k_B is Boltzmann's constant, c is the concentration of repeating units (monomers), f is the fraction of monomers with a free counterion and ξ is the correlation length or mesh size which scales with concentration as $c^{-1/2}$. The Manning and Katchalsky models multiply the first term in Eq. 1 by a constant of $\simeq 0.5$, but this is not important for the discussion here.

Figure 1 plots the osmotic pressure of polystyrene sulfonate in water as a function of polymer concentration. The linear dependence expected by the first term of Eq. 1 is observed to hold well and only at very high concentrations the $\xi^{-3} \propto c^{1.5}$ appears relevant.[8] The black line corresponds to $f \simeq 0.2$ which aligns well with other estimates for the fraction of free counterions of NaPSS in water from counterion activity measurements or electrical conductivity.

One consequence of the high osmotic pressure observed in figure 1 is that low-salt polyelectrolytes solutions are expected to be highly incompressible systems where long-ranged concentration fluctuations are strongly suppressed. Because of this, polyelectrolytes have long been predicted to scatter weakly in the low-q regime.[5,20–22] Experimentally, however, with some exceptions,[23–25] the low-q region of the scattering function of polyelectrolyte solutions displays a large upturn. Several mechanisms have been proposed that predict aggregation in polyelectrolyte solutions and thus to strong scattering at low q. However, it is not clear how such aggregation can be reconciled with the characteristically low osmotic compress-

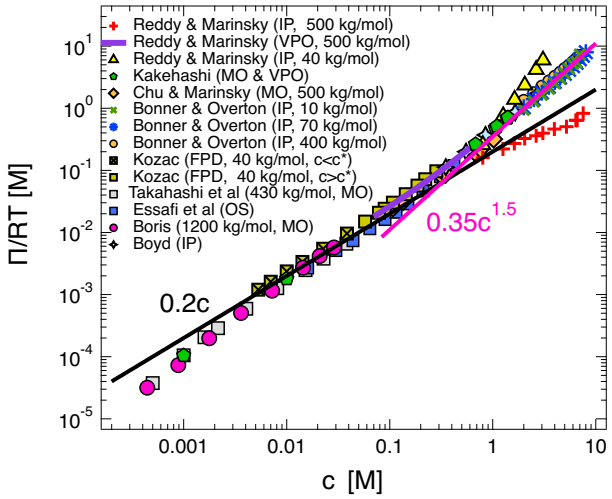

FIG. 1. Osmotic pressure of NaPSS as a function of concentration. The black line corresponds to Eq. 1 with $f = 0.2$. The purple line as best fit to the high concentration region. Data are from refs. [9–18], as indicated on the legend. Letters inside brackets correspond to measuring method: IP = isopiestic method, VPO = vapour pressure osmometry, MO = membrane osmometry, FDP = freezing point depression osmometry, OS = osmotic stress.

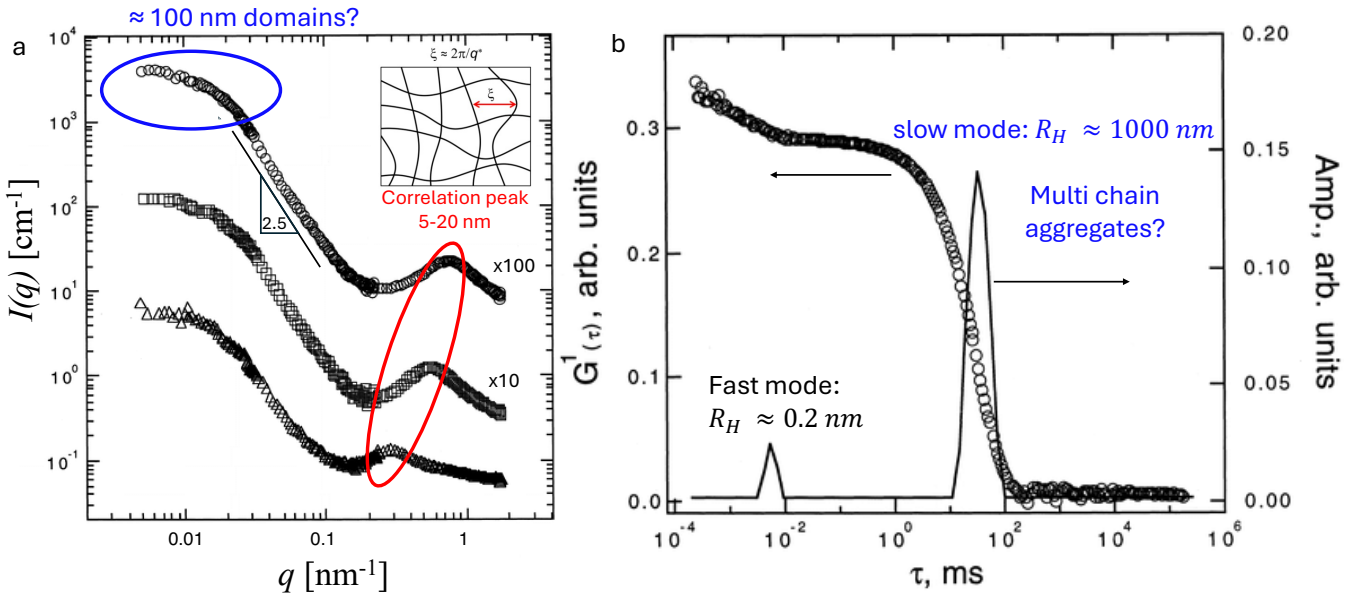

FIG. 2. Scattering properties of quaternised P2VP in aqueous solutions without added salt. **a:** combined SLS and SANS intensity for $c = 3, 15 and 30$ g/L. The two highest concentrations are shifted by factors of 10 and 100, as indicated on the plot. The SLS data were shifted vertically to match the SANS data.[a] The correlation peak observed at intermediate q corresponds to the mesh size of the polymer solution, depicted schematically on the inset. The low q upturn follows a power-law of $I(q) \sim q^{-2.5}$ before plateauing for $q \lesssim 0.01$ nm^{-1}. Guinier analysis of the low-q region gives characteristic sizes of $\simeq 100$ nm. **b:** The dynamic light scattering field correlation function for the 30 g/L solution displays a clear bimodal profile. The fast mode with an *apparent* size of 0.2 nm arises from the diffusion of the free counterions, whose motion is coupled to that of the backbone. The slow decay corresponds to size of $\simeq 1$ μm. Figure adapted from [19].

[a] The cm^{-1} unit therefore strictly applies only to the SANS data.

ibility of these systems. Properly stated, the low$-q$ problem is not simply that polyelectrolyte solutions scatter strongly at low q, but that this occurs in solutions exhibiting a very large osmotic pressure, which should correspond to a very small compressibility.

A good example of the puzzling experimental results is shown in figure 2a, which plots the small angle neutron scattering (SANS) and light scattering intensity of quaternized poly(2-vinyl pyridine) in aqueous solutions.[19] In the intermediate q range the scattering function displays a correlation peak associated with the mesh size of the polymer solution. This peak was first predicted by de Gennes et al[5] and subsequently observed in many experimental studies.[26–34] At still lower q, however, the intensity increases sharply, following a power law of approximately $I(q) \sim q^{-2.5}$ before reaching a plateau at very small scattering vectors. Guinier analysis of this region yields characteristic length scales on the order of $\sim 80 - 90$ nm, which are much larger than the mesh size of the semidilute solution.

Dynamic light scattering measurements provide additional information about this anomalous low-q scattering. As shown in figure 2b, the field correlation function exhibits a clear bimodal decay consisting of a fast and a slow relaxation mode with characteristic times $t_{\text{fast}} \simeq 5$ μs and $t_{\text{slow}} \simeq 30$ ms. An apparent diffusion coefficient can be calculated as $D_{\text{app}} = \Gamma_i / q^2$, where Γ_i is the mean inverse relaxation time. From this apparent diffusion coefficient, the hydrodynamic radius can be estimated using the Stokes–Einstein equation:

$$R_H = \frac{k_B T}{6\pi \eta_s D_{\text{app}}} \tag{2}$$

where η_s is the viscosity of the solvent.

In applying Eq. 2 it is implicitly assumed that the diffusing species experiences a hydrodynamic drag proportional to the solvent viscosity. While this assumption is likely to hold for the diffusion of small ions or short sections of the polymer chain, it is less appropriate for the entities responsible for the low-q upturn and the slow mode. These objects have dimensions much larger than the mesh size of the polymer network, and therefore the hydrodynamic drag they experience is likely to be closer to the *solution* viscosity rather than the solvent viscosity.[35–37] This conjecture is supported by three observations. 1) the static size of the aggregates obtained from Guinier fits to the data in figure 2a is approximately $\simeq 100$ nm, which is much smaller than the apparent hydrodynamic radius of ~ 1 μm obtained from Eq. 2 when the solvent viscosity is used. The solution viscosity for the sample in figure 2b can be estimated as $\simeq 10$ mPa s based on measurements by Dou[38] for a P2VP derivative of similar degree of quaternization.[39] 2) when filtration is used, the largest species in solution are limited by the filter pore size. Lopez and Richtering[40] showed that for various salts of carboxymethyl cellulose the hydrodynamic radii of the slow mode calculated using the solvent viscosity were much larger than the filter pore size. Replacing

η_s by the solution viscosity in Eq. 2 produced values consistent with the filtration limit. 3) Data by Behra *et al.* showed that ratio D_{app}/η_{sp} for NaCMC solutions is nearly concentration independent, as expected for constant size object whose diffusion is slowed down by the increasing viscosity of more concentrated solutions.

The fast mode corresponds to the diffusion of counterions, whose motion is coupled to that of the polymer backbone.[41–43] It is found to be independent of polymer molar mass and weakly dependent polymer concentration in the semidilute regime[44,45] but dependent on the size and valence of the counterion[40,46,47] and the charge density[42,48,49] of the chain.

The slow mode, as discussed above, is expected to arise from the same entities responsible for the low-q upturn. It displays a complex dependence on polymer molar mass, concentration and added salt type and content.[44,45,50,51] The molar mass and concentration dependence of the hydrodynamic size is considerably more complex than that of the static size, likely because the hydrodynamic size is influenced by the solution viscosity, as discussed above. Various interpretations for its origin have been proposed.[52,53] Although the proposed mechanisms differ, they can be broadly grouped into two classes: multi-chain domains,[19,43,47,54–60] and extraneous species such as dust, undissolved polymer, or other residues.[61–63]

Neither interpretation fully explains the available observations. The dust hypothesis is difficult to reconcile with several experiments. Sedlak showed that the slow mode reappears when filtered solutions are allowed to stand for extended periods.[64] Similarly, the amplitude and diffusion coefficient of the slow mode was found by Sedlak to display slow kinetics, which is difficult to explain by the dust/residue hypothesis.[65] In addition, the slow mode appears when a weak polyacid is charged *in situ* by increasing the pH,[66,67] which cannot easily be attributed to contamination. Russo and co-workers[59] demonstrated using a dialysis–DLS setup that the slow mode disappears upon salt addition and reappears when the salt is removed. Such reversible behaviour is inconsistent with a dust-based explanation. The multi-chain domain hypothesis faces two difficulties: First, as discussed above, salt-free polyelectrolyte solutions have a very high osmotic pressure, which strongly suppresses long-range concentration fluctuations. Any large-scale concentration heterogeneity would generate a substantial osmotic pressure difference between concentrated and dilute regions, driving rapid homogenisation of the system. Second, the macroscopic properties of polyelectrolyte solutions such as solution viscosity do not show any properties that suggest the presence of large aggregates of chains. Measurements of chain self-diffusion by fluorescence correlation spectroscopy[68–70] or pulsed-field gradient NMR[71–73] also fail to show any slow dynamics that would be expected from the presence of multi-chain aggregates.

Recently, Sedlak[74] argued that two types of entities are responsible for the slow mode. The first arise from hydrophobic molecules, which are solubilised by neutral polymers but when the backbone is charged they are released into solution and aggregate up to a critical size where they become stable due to the surface charge of the droplet. This mechanism can explain the generation of the slow mode upon polyelectrolyte charging without involving macro-ion domains.

Simulation studies often do not observe an upturn in the structure factor[75–78] and the scattering function is observed to monotonically decrease with decreasing q. An exception to this is the work of Chremos and Douglas,[79–82] who find that a low$-q$ upturn is observed when the affinity between the counterions and the solvent exceeds a critical threshold.

Finally, we note that excess scattering in the low$-q$ region is not a feature restricted to polyelectrolytes but has also been observed for other polymers in polar solvents, see for example the work of Hammouda and co-workers: [83–87] These results show some similarities with the phenomenology of polyelectrolyte solutions[88] such as the sensitivity of the amplitude and relaxation time of the slow decay to filter size, as well as similar power-law dependences for the low$-q$ upturn, but it is unknown if the origin of both types of clusters is the same.

Regardless of the origin of the low-q upturn, it would be useful to know what the scattering function of a polyelectrolyte solution looks like in its absence. One reason for this is that the zero-angle scattering intensity is related to the osmotic compressibility of two-component solutions.[89] Measuring $I(0)$ therefore provides a way of determining the osmotic compressibility (the derivative of the osmotic pressure with respect to concentration). Most commercially available osmometers today use the freezing point depression method and are designed for aqueous solutions.[90] By contrast, light scattering measurements can generally be performed in organic solvents regardless of volatility or chemical harshness. The earliest example of using the zero-angle scattering intensity to determine the fraction of free counterions in salt-free polyelectrolyte solutions is by Alexandrowicz,[23] who noted that 'proper clarification *[by centrifugation]* proved to be of crucial importance, omission of it leading to possible errors of several hundred per cent' A more recent example is by Saha et al[24,25], who measured the light scattering properties of poly(2-vinyl-pyridine) with varying degree of quaternisation in 1-propanol solution. In their case, no slow mode/low$-q$ upturn was observed for the solutions.

In this work we show that the low-q upturn can be largely removed by filtration through sufficiently small pores and that the remaining contribution of the slow mode can be separated using analysis of the dynamic light scattering autocorrelation function. Once this contribution is removed, the resulting scattering intensity agrees with theoretical expectations for salt-free polyelectrolyte solutions and provides a direct way of determining the osmotic compressibility, and from there the osmotic pressure and the fraction of free counterions of polyelectrolyte solutions. A major advantage of using light scattering instead of osmometry is that light scattering can be used in non-aqueous solvents, which are difficult to handle with most osmometric techniques

II. EXPERIMENTAL METHODS

Materials: The sodium carboxymethyl celluloses used in this study were purchased from Sigma-Aldrich and have DS

= 1.3, see refs. [40,91] for details of the DS and molar mass characterisation. The preparation of the TBA salt of CMC is the same as in refs. [92,93]. Dialysis membranes with MWCO 10kDa were obtained from SpectraPor. Capillaries for SAXS experiments were purchased from Hampton Research (US). The sodium salt of poly(γ-glutamic acid) (NaPGA) was purchased from MarkNature (grade: Purity 99%, Cosmetic Grade, produced by bacterial fermentation). The powder was dissolved in water, extensively dialysed against DI water to remove salt impurities. The magnesium salt of PGA was prepared by adding a 40-fold molar excess of $MgCl_2$ to an aqueous solution of NaPGA followed by extensive dialysis against DI water. After dialysis, the polymers were freeze dried and the dried powder was used to prepare solutions.

Small Angle Neutron Scattering: SANS experiments were carried out at two beamlines: the SANS2D instrument at the ISIS neutron source (Didcot, UK) and the JRR-3 instrument at J-PARC (Tokai, Japan). The sample-to-detector distances were 4m for both instruments. The SANS-2D experiments were carried out using a white beam. For the JRR-3 experiments $\lambda = 7$ Å was used. Samples were loaded into quartz cells and data were reduced using the software provided by the respective facilities.

Small Angle x-ray Scattering: SAXS experiments were carried out at the Spring-8 synchrotron facility, beamline BL40. The sample to detector distance was 1 or 2 m and x-ray energy was 12.6 keV. Samples were loaded into $\simeq$ 2 mm quartz capillaries and sealed using a glue gun to prevent evaporation. Transmission and scattering spectra were collected simultaneously. The data were radially averaged and the capillary was subtracted according to standard procedures.

Static and dynamic light scattering: Dynamic light scattering on the TBACMC solutions were carried out on an ALV CGS-3 goniometer system with two detectors at the same angle and a 632.8 nm He-Ne laser. The cross-correlation mode was used for all measurements. Samples were measured in disposable glass cuvettes (diameter = 8 mm) and prepared using the same procedure as for the SLS experiments. Measurements were carried out at scattering angles from 30° to 150° in 10° increments. Static light scattering measurements were performed using an instrument from SLS-Systemtechnik (Denzlingen, Germany). Two diode lasers with wavelengths $\lambda = 407$ nm and $\lambda = 640$ nm were used. Measurements were carried out in quartz cuvettes (20 mm diameter, Hellma Analytics). Before sample loading, the cuvettes were cleaned by rinsing with freshly distilled acetone in a modified distillation column for at least 30 minutes. Light scattering from solutions of NaPGA and MgPGA were measured on a LS-II combined static and dynamic light scattering instrument from LSi (Switzerland) using the cross-correlation mode with two detectors at the same angle. The laser has a wavelength of 638 nm and a power of 75 mW. The scattering intensity was recorded at 40, 90, 120 and 150 degrees for a duration of several minutes per angle. Calibration of static light scattering into an absolute scale was done using toluene as the standard.[94]

Refractive index increment: The refractive index of TBACMC was measured using a differential refractometer from SLS-Systemtechnik instrument (Denzlingen, Germany) equipped with a 633 nm diode laser. Samples were loaded through a 0.8 μm syringe filter into a 12.5 mm $\times$ 12.5 mm cuvette containing two chambers separated by a 45° prism. One chamber was filled with water and the other with the sample. Before each measurement the cuvette was cleaned with water and acetone and dried with compressed air. The sample temperature was controlled using a circulating water bath with a resolution of 0.1 °C. Refractive index increments of the various polyglutamic acid salts were measured using a RA-620 refractometer from KEM instruments (Japan) with a wavelength of 589.3 nm. The instrument records n with an accuracy of $\pm$ 0.00002.

Freezing point depression osmometry: An Osmotech XT from Advanced Instruments (US) was used for all measurements. The instrument is designed to handle solutions of high viscosity, which are often problematic with FDP osmometers. The instrument determines the freezing point of the test solution and outputs the osmolarity, calculated as $c_{osm} = K_f \Delta T$, where ΔT is the change in freezing temperature with respect to water and $K_f = 1.86$ M/K is the cryoscopic constant of water.[95] The osmometer was checked against standards provided by the manufacturer with osmolarities of 0, 100 and 289 mM.

Electrical conductivity: Conductivity measurements were performed using a SevenExcellence pH/conductivity meter (Mettler Toledo). An InLab741 conductivity probe with two stainless steel electrodes was used to measure conductivities in the range 0.001–500 μS cm^{-1}. An InLab710 conductivity cell with four platinum electrodes was also used, covering the range 0.01–500 mS cm^{-1}. Samples within the overlap region (100–500 μS cm^{-1}) were measured with both probes to verify consistency of the results. The InLab741 probe was calibrated using a 100 μS cm^{-1} standard solution equilibrated to 25°C in a water bath. The InLab710 conductivity cell was calibrated in the same manner using a 1413 μS cm^{-1} standard solution. Solutions were placed in plastic vials, the conductivity probe, which has an integrated temperature sensor, was inserted and the solution was equilibrated to 25 $\pm$ 0.1 °C before the conductivity value was recorded.

Thermogravimetric analysis: Thermogravimetric analysis (TGA) was performed using a Discovery TGA 550 (TA Instruments) under a nitrogen flow of 50 mL min^{-1}. NaPGA and Mg samples were placed in clean, tared 100 μL platinum TGA pans without lids. The samples were first heated to 120 °C and held for 1 h, then heated from 120 to 420 °C at a rate of 10 °C min^{-1}. The water content of the PGA was determined from the mass loss in the first stage (25–120 °C).

III. BACKGROUND THEORY AND DATA ANALYSIS

A. Polyelectrolyte conformation and counterion condensation

Polyelectrolytes in dilute salt-free or low-salt solutions are predicted to adopt highly stretched conformations, with an

end-to-end distance proportional to their degree of polymerisation, N.[4,6] The main experimental evidence supporting this prediction is the observed N^{-2} dependence of the overlap concentration, c^*.[27,53,96,97] Above the overlap concentration, chains interpenetrate and form a mesh with characteristic size ξ, known as the correlation length. The scaling theory predicts the correlation length to be:

$$\xi = \left(\frac{B}{bc}\right)^{-1/2} \tag{3}$$

where b is the size of the monomer, c the concentration of such monomers[98] and B is the stretching parameter which is equivalent to the ratio of the fully extended length of the monomers inside a correlation blob relative to the end-to-end distance of the blob.[99] When the chain is fully stretched inside the correlation blob, as is usually the case for semiflexible polysaccharides[100,101], B is approximately equal to one. For flexible polyelectrolytes values of $B \simeq$ 2-5[38,102–104] are common.

Oosawa and Manning[1,3,105,106] derived for salt-free polyelectrolytes in the infinite dilution limit the theory of counterion condensation. In brief, when the charge density exceeds $e/(Z_C l_B)$, where Z_C is the counterion valence and l_B is the Bjerrum length of the solvent, given by: counterions are trapped (condensed) in the vicinity of the polymer backbone and do not contribute to charge transport or osmotic properties of the solution. The Bjerrum length is the lengthscale at which Coulombic attraction between a pair of oppositely charged monovalent counterions equals their thermal energy:

$$l_B = \frac{e^2}{4\pi\varepsilon_0\varepsilon_r k_B T}$$

where ε_0 is the vacuum permittivity, ε_r the relative permittivity of the solvent and e the unit of electrostatic charge. Solvents with lower dielectric dielectric constants have large Bjerrum length and polyelectrolytes are predicted to exhibit lower effective charges, which is qualitatively supported by experiments.[53,93,107,108]

While the counterion condensation theory was derived for isolated chains, Wandrey et al showed that the Oosawa-Manning limit (one charge per Bjerrum length for monovalent counterions) applies in the semidilute regime,[109,110] in agreement with the condensation model of Tang and Rubinstein.[111]

Since only free counterions contribute to the osmotic pressure of a polyelectrolyte solution, we can write:

$$\frac{\Pi}{k_B T} = g^* f c \tag{4}$$

where we neglect the contribution of polymer-polymer contacts (i.e., the ξ^{-3} in Eq. 1). g^* is the activity coefficient of a free counterion. The theory of Manning predicts a transition from $g^* = 1$ for weakly charged polyelectrolytes to $g^* = 1/2$ for strongly charged polyelectrolytes, in agreement with Lifson-Katchalsky model.[20] Oosawa's model, which treats free counterions as non-interacting with the polymer backbone predicts $k_B T$/free counterion ($g^* = 1$), in agreement with the scaling theory.

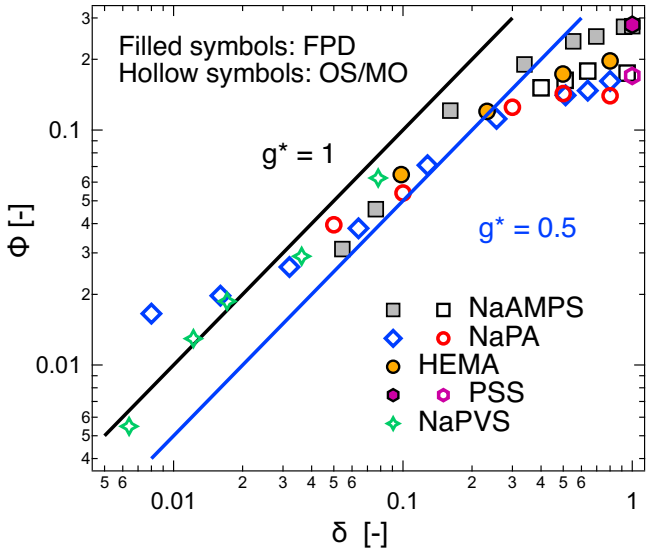

FIG. 3. Osmotic coefficient of flexible polyelectrolytes as a function of degree of ionisation/ionic group fraction. Data are from refs. [10,23,112–116]. For PSS, a hydrophobic polyelectrolyte, only the data for fully sulfonated ($\delta = 1$) values are included. Black and blue lines correspond to $g^* = 1$ and $g^* = 1/2$ respectively. Filled symbols are for measurements by freezing point depression (FPD) and hollow symbols are for measurements made by membrane osmometry (MO) or osmotic stress (OS). Osmotic stress here includes the traditional method using dialysis bags[10] and also gel osmometry.

Experimental data for the osmotic coefficient of semidilute flexible polyelectrolytes as a function of the fraction of monomers with an ionic group (δ) are plotted in figure 3. The data display considerable scatter but they suggest a transition from $g^* \simeq 1$ at low charge densities to $g^* \simeq 1/2$ near the onset of counterion condensation ($\delta \simeq 0.3$), which is identified as the point at which the osmotic coefficient becomes independent of the bare (chemical) charge density. For the vinylic polyelectrolytes considered here, the monomer size is $b \simeq 2.5$ Å. The distance between charged groups is therefore b/δ, which at $\delta \simeq 0.3$ gives $b/\delta \simeq 8$ Å. This value is close to the Oosawa-Manning condensation threshold, $b/\delta \simeq l_B$, where the Bjerrum length in water is $l_B \simeq 7.1$ Å. In the following, for simplicity, we will use $g^* = 1$ to estimate f from osmotic pressure data.

B. Static light scattering

The intensity of scattered light is usually expressed in terms of the excess Rayleigh ratio (ΔR), which is related to the total structure factor $S(q)$ as:

$$\Delta R(q) = K\rho_{pol}^2 N_A S(q) \tag{5}$$

where ρ_{pol} is the polymer density and K is the optical contrast constant, given by:

$$K = \frac{4\pi^2 n_0^2}{N_A \lambda^4}\left(\frac{dn}{dC}\right)^2$$

where $\frac{dn}{dC}$ is the refractive index increment of the polymer in the solvent, n_0 the refractive index of the solvent and λ is the wavelength of the laser.

In the zero-angle limit, $S(q)$ is related to the osmotic compressibility of a solution as:

$$S(0) = k_B T \phi \frac{d\phi_p}{d\Pi} \tag{6}$$

where $\phi_p = C/\rho_{pol}$ is the volume fraction of the polymer.

Approximating the osmotic pressure of a salt-free polyelectrolyte solution as $k_B T$ per counterion (Eq. 4 with $g^* = 1$) and using eq. 5:

$$\frac{KC}{\Delta R(0)} = fM_0 \tag{7}$$

where M_0 is the molar mass of a monomer. In terms of the Zimm plot, the apparent molar mass of the polymer is $M_{app} = fM_0$.

Equation 7 holds as long as Eq. 4 gives a correct description of the osmotic pressure. If non-linear terms in c are added to Eq. 4, then Eq. 7 must be corrected accordingly, but since f is found to be concentration-independent from conductivity and osmotic pressure data in the range where SLS/DLS is used, we judge Eq. 4 to be accurate.

In a SLS experiment, ΔR is measured as a function of scattering angle θ and can be extrapolated to zero angle to obtain $\Delta R(0)$. If the refractive index increment is known, Eq. 7 can be used to estimate f. Equation 7 shows that the scattering intensity of a salt-free polyelectrolyte at zero angle corresponds to an apparent molar mass equivalent to a polyelectrolyte segment with one effective charge.

C. Dynamic light scattering

The solution to use dynamic light scattering (DLS) to split the total scattering signal into the contributions from the slow and fast modes. The primary result of a dynamic light scattering experiment is g_2, the intensity correlation function, which is related to field correlation function g_1 by the Siegert relation:

$$g_2(\tau) = 1 + \beta g_1^2(\tau)$$

where β is a coherence factor.

The field autocorrelation function of a salt-free polyelectrolyte solution can be modelled by a sum of two cumulant expansions:

$$\begin{aligned} g_1(\tau,q) = A_1(q) e^{-\Gamma_1(q)\tau}\left(1 + \frac{\mu_{2,1}\tau^2}{2}\right) \\ + A_2(q) e^{-\Gamma_2(q)\tau}\left(1 + \frac{\mu_{2,2}\tau^2}{2}\right) \end{aligned} \tag{8}$$

where τ is the correlation time, A_1 and A_2 are the amplitudes of the two modes, Γ is the mean inverse relaxation time or first cumulant, μ_2 is the second cumulant, which is related to the variance of the distribution of relaxation times and the subscripts 1 and 2 refer to the fast and slow mode respectively.

The total excess Raleigh ratio (ΔR) can be split into fast and slow mode contributions as follows:

$$\Delta R_{fast}(q) = \frac{A_1(q)}{A_1(q) + A_2(q)} \Delta R(q) \tag{9}$$

$$\Delta R_{slow}(q) = \frac{A_2(q)}{A_1(q) + A_2(q)} \Delta R(q)$$

D. Polyelectrolyte conducitivity

The conductivity of a salt-free polyelectrolyte solution with monovalent counterions is calculated by the model of Colby et al as:[117,118]

$$\frac{\sigma}{c} = f\left[\lambda_0 + \frac{N_A^2 c \xi^2 e^2 ln(\xi/D)}{3\pi\eta_s}\right] \tag{10}$$

where η_s is the viscosity of the solvent, λ_0 the limiting specific molar conductance of the counterion: 5.0 for Na^+, 5.3 for Mg^{2+} and 3 for TBA^+ mSm^2/mol, all in water. For Na^+ in ethylene glycol, we assume the Walden product in EG and water is the same and estimate a mobility of 0.17 mSm^2/mol.[119] ξ is the correlation length, D the cross-sectional diameter of the chain, taken to be 7 Åfor both CMC and PGA.

If the conductivity and correlation length are known, equation 10 allows the fraction of free counterions to be estimated at a given concentration.

IV. RESULTS AND DISCUSSION

The light and x-ray scattering data along with the conductivity, osmotic pressure and TGA results are tabulated in the supporting information. All data are for 25 °C unless otherwise indicated.

A. Refractive index increment, electrical conductivity and freezing point depression osmometry

TABLE I. Refractive increment of CMC and PGA salts. Values for $\lambda = 589.4$ are measured using the KEM refractometer and value for $\lambda = 633$ nm are using the SLS-Systemtechnik one. [a] Behra et al measured dn/dc using an Abbe refractometer and their value presumably corresponds to white light.

Polymer	Solvent	λ [nm]	dn/dc [mL/g]	source
TBACMC	water	633	0.168	This work
NaCMC	water	–[a]	0.171	[120]
NaPGA	water	589.4	0.2	This work
NaPGA	ethylene glycol	589.4	dn/dc	This work
MgPGA	water	589.4	dn/dc	This work

The refractive index increments of the various polymer salts studied are given in table I. For this work, we ignore the wavelength dependence of the refractive index of the polymers in the range of 589-638 nm, which is quite small.[121]

Conductivity data for the TBACMC polymer used here were reported in an earlier study.[93] Conductivity data NaCMC of various degrees of substitution are also available are also available from our work[101] and that of of Ray et al[122]. The electrical conductivity of NaPGA in water and ethylene glycol and of MgPGA in water are compiled in table S2.

B. Correlation length of PGA

Correlation length data for NaCMC[33,34,101,123] and TBACMC[92] in water are available from previous studies. These consistently show a stretching parameter of $B \simeq 1$, corresponding to locally stretched conformations. Correlation length data for NaPGA in water and ethylene glycol and for MgPGA in water were obtained from SAXS measurements on solutions without added salt. Representative data are shown on figure 4. The scattering functions of PGA solutions display a peak with the maximum at q^*, examples for NaPGA and MgPGA in water are shown in figure 4a and 4b respectively. The correlation length is calculated as: $\xi = 2\pi/q^*$. For MgPGA the peak morphs into a shoulder at high concentrations. For samples displays a shoulder, the position of q^* is obtained by fitting two power-laws at high and low q and taking q^* as the intercept. This behaviour has been observed for other systems, see for example [100]. For CMC, the sodium salt displays a correlation peak over the 0.01-0.2 M concentration range. The magnesium salt displays correlation shoulders over the same concentration range. The sharpness of the peaks decreases in the order NaPGA/water $>$ NaPGA/EG $>$ MgPGA/water, see the supporting information. This corresponds to the order in which the effective charge density of the chain decreases. Less charged chains lead to weaker electrostatic correlations and a decrease in peak sharpness.

The correlation length for NaPGA and MgPGA in water and for NaPGA in ethylene glycol is plotted as a function of concentration in figure 4c. The concentration exponent ($\simeq -0.4$) is around 20% smaller than the theoretical value of $-1/2$ (Eq. 3). The Oosawa-Manning theory expects the effective charge density of the chain to be a proportional to $1/(Z_C l_B)$, which is approximately the same for NaPGA in EG and MgPGA in water. For two systems with the same effective, the scaling theory expects the value of B (and therefore of the correlation length) to be the same if the solvent quality does not change. The correlation length of MgPGA in water is significantly larger than NaPGA in EG, corresponding to more collapsed chains in the former. According to the scaling theory this means that water is a worse solvent for the PGA backbone that EG, which would also explain why NaPGA has a similar correlation length in water and EG despite having a larger effective charge in water. An alternative explanation is that the Mg^{2+} ions created intra-chain bridging interactions leading to a local collapse of the chain. This interpretation is discussed in more detail after considering the measurements of the polyelectrolyte effective charge.

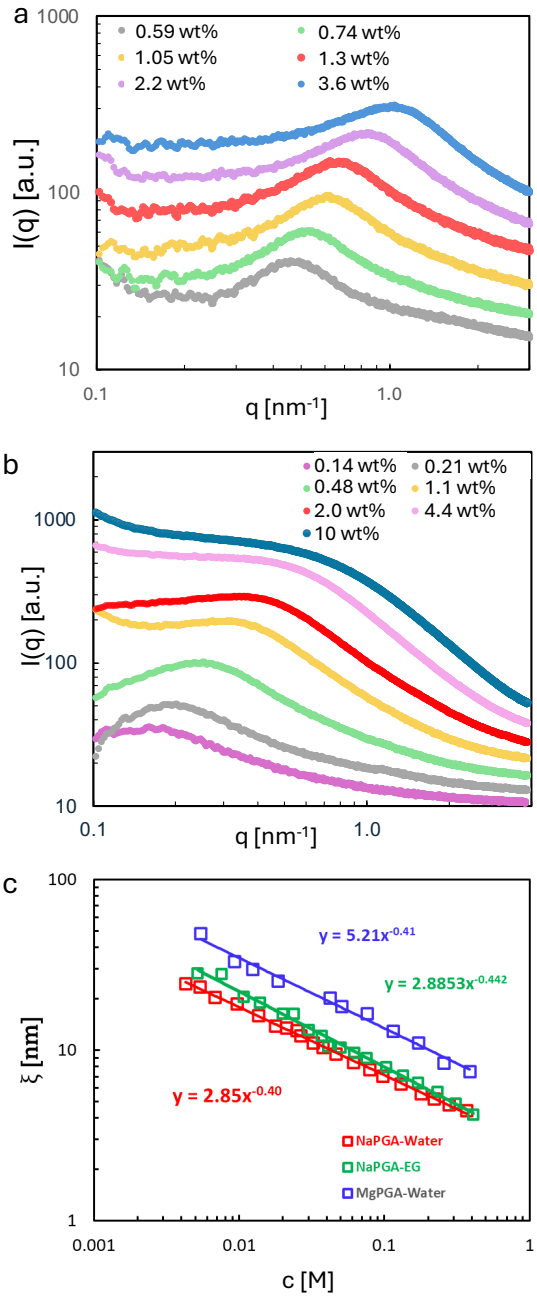

FIG. 4. a: SAXS curves for NaPGA in water, data are shifted vertically for clarity. b: same as part (a) but for MgPGA in water. c: correlation length $\xi = 2\pi/q^*$ as a function of concentration for NaPGA and MgPGA in water and for NaPGA in ethylene glycol. Lines are best-fit power-laws.

C. Influence of filtering

The relative amplitude of the slow mode is known to decrease upon filtration, with the reduction becoming more pro-

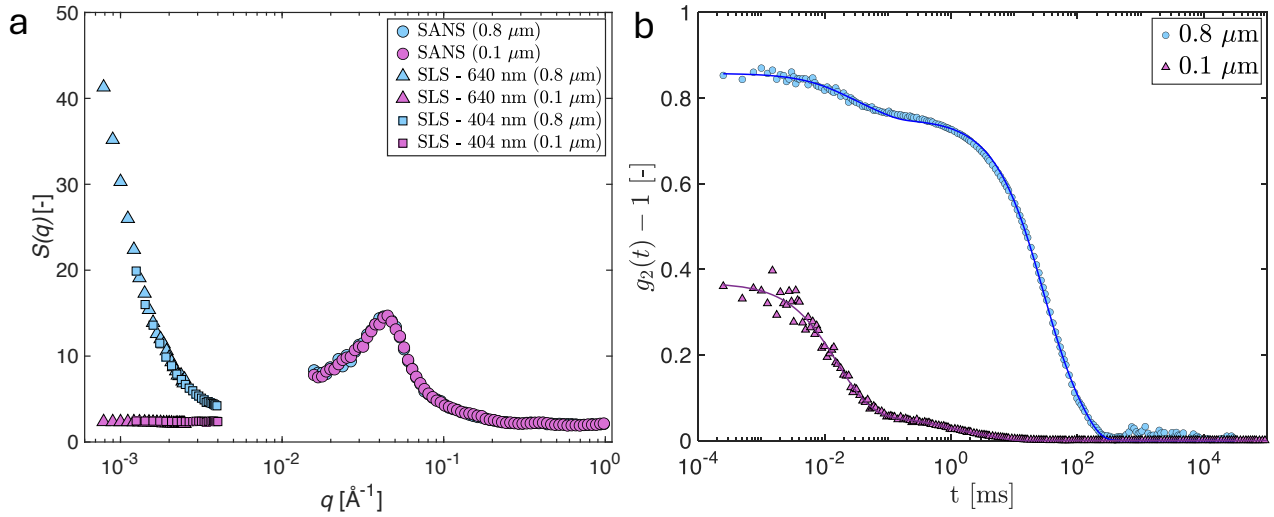

FIG. 5. a: SLS and SANS intensities of $c = 0.02$ M TBACMC solutions in D_2O without added salt. The solutions have been passed through a 0.1 μm filter (purple symbols) or through a 0.8 μm filter (blue symbols). The SLS data were collected at two different wave-lengths to extend the range of q. b: DLS intensity autocorrelation functions for the same solutions as in part a. The lines are a fit to a bimodal decay function. Note the large drop in the intensity of the low$-q$ upturn and slow mode upon decreasing filter size. The decay time of the fast mode does not change with filter size.

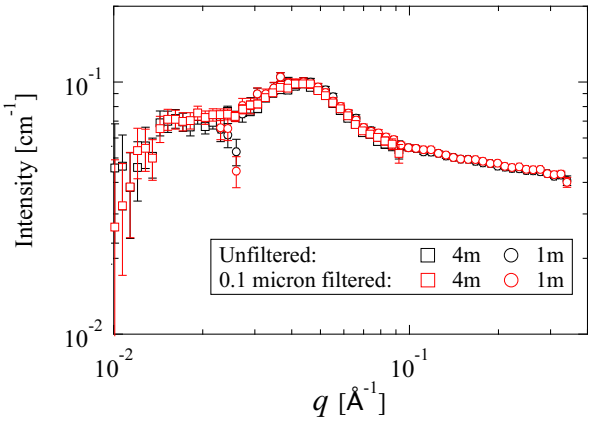

FIG. 6. Comparison of SANS intensity for unfiltered and 0.1μm-filtered 0.02 M TBACMC solution in D_2O. Circles and squares correspond to 1 m and 4 m sample to detector distances. Data were collected at 8m but found to be to noisy for analysis.

nounced as the filter pore size decreases.[64] In general, when applying Eq. 8, if $A_{\text{slow}} \gg A_{\text{fast}}$, it becomes difficult to accurately isolate the contribution of the fast mode to the total scattering signal. Filtering is therefore beneficial for the accurate determination of f using light scattering. For this reason, we begin by examining the influence of filter pore size on the properties of tetrabutylammonium carboxymethyl cellulose (TBACMC) solutions.

Figure 5 compares the static structure factor of two TBACMC solutions in D_2O ($c = 0.02$ M) filtered through pore sizes of 0.1 and 0.8 μm. The low-q range was measured by light scattering, while the mid- and high-q ranges were measured by SANS. The structure factor is shown rather than the scattering intensity in order to remove the influence of scattering contrast.

The correlation peak centered around $q \simeq 0.045$ Å^{-1} is unaffected by filtration. This is also evident in figure 6, which shows the mid-q scattering intensity of a TBACMC solution before filtering and after filtration through a 0.1 μm pore-size filter. The insensitivity of the scattering around the peak position indicates that the mesh size of the semidilute polymer network remains unchanged. The result also suggests that filtration does not remove a significant number of polymer chains, since such removal would reduce the scattering intensity.[124] This result is consistent with the insensitivity of the solution viscosity to filter pore size reported previously for CMC solutions.[40] As discussed in the introduction, one puzzling aspect of the multi-chain domain interpretation of the slow mode/low$-q$ upturn is that such domains appear to have little influence on the rheological or other macroscopic properties of the solution. The data in figures 5–6 reinforce this point. Although the magnitude of the slow mode and the low-q upturn vary strongly with filtration, the correlation length, which controls chain conformation and dynamics, remains unchanged.

The reduction of the low-q upturn and the slow mode when filtering through 0.1 μm filters instead of 0.8 μm filters is consistent with the removal of the entities responsible for these features. The decay time of the fast mode is unaffected by filter size (see figure S1), as expected since it is associated with counterion diffusion, a local property. In contrast, the slow mode becomes less prominent when smaller pore-size filters are used, and its apparent hydrodynamic size decreases, presumably because the maximum size of the remaining entities is limited by the filter pore size.

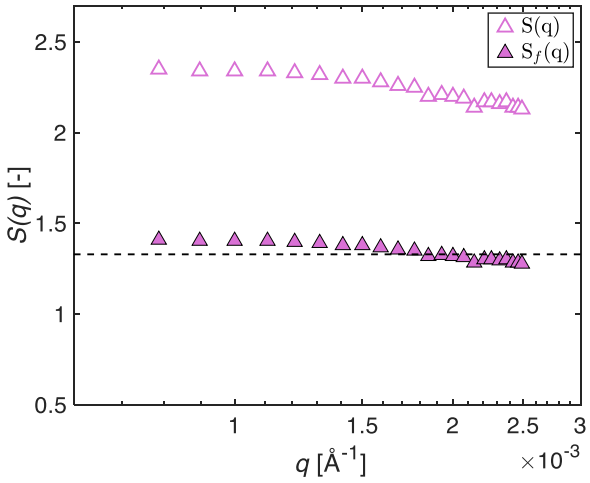

FIG. 7. Total structure factor (hollow symbols) and fast component (full symbols) of the structure factor for 0.1 μm-filtered solution of TBACMC in D_2O.

Figure 7 plots the total structure factor and the fast mode contribution to the total structure factor for the 0.1 μm-filtered solutions. The splitting of the scattering intensity is calculated using Eqs. 8 and 9. Both quantities display a weak $q-$dependence, which may or may not be an experimental artefact.

D. Comparison of SLS/DLS and conductivity methods

1. TBACMC, DS $\simeq$ 1.3

The fraction of monomers with a dissociated counterion for TBACMC in water were evaluated from scattering and electrical conductivity measurements in ref. [93] to be $\simeq 0.6$. This is relatively close to the value of 0.66 evaluated from the fast mode contribution in figure 7.

2. NaCMC, DS $\simeq$ 0.9

Behra et al[120] carried out a careful light scattering study of sodium carboxymethyl cellulose with DS $= 0.85$. The refractive index increment of their sample was reported as 0.17 mL/g. The authors used rather large filter pore sizes of $1-1.6\mu$m and split the total scattering signal into fast and slow components following a procedure similar to the one outlined above but using a stretched exponential for the slow mode decay instead of a cumulant expansion. Using the ΔR_{fast} and dn/dc value reported by Behra et al, the values of f are plotted as a function of concentration in figure 8. The values of f are seen to be concentration independent, as required for Eq. 7 to apply. These values are compared with conductivity estimates of f for a similar NaCMC polymer (DS $\simeq 0.9$) based on the data of Ray et al, see [101] for details of the calculation of f. Both datasets are seen to agree well.

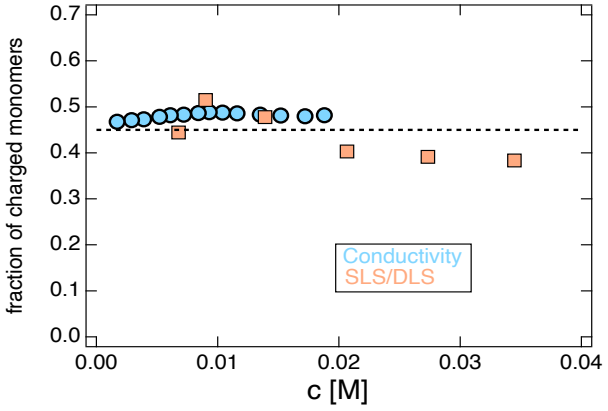

FIG. 8. Fraction of free counterions as a function of concentration for NaCMC in water evaluated from conductivity, using data from ref. [122], and SLS/DLS, using data from [120]. Dashed line is the average value from both techniques: $f \simeq 0.45$.

3. NaPGA and MgPGA

The values of f estimated from freezing point depression, conductivity/SAXS (Eq. 10 with ξ measured by scattering) and SLS/DLS for sodium salt of polyglutamic acid (NaPGA) are plotted as a function of concentration in figure 9a. For ethylene glycol solutions, the osmotic pressure method could not be applied. In water, all three methods are seen to agree well and give a value of $f \simeq 0.48$, in modest agreement with the Oosawa-Manning prediction of $f = l_B/b \simeq 0.7$, where $l_B = 0.71$ nm is the Bjerrum length of water and $b \simeq 0.5$ nm is the projected monomer length.[125]

The comparison of NaPGA and MgPGA shows that the divalent counterion produces a much lower fraction of dissociated counterions, consistent with earlier observations for PSS.[104,126] The strong decrease in f ($\simeq \times 5$) is not observed for polysaccharides such as CMC, alginate, arabic gum or chondroitin sulfate,[101,127–131] where the Oosawa–Manning prediction, namely that f is inversely proportional to the counterion valence, is clearly observed. A possible explanation is that the greater intrinsic stiffness of polysaccharide backbones makes their local conformation relatively insensitive to counterion valence. By contrast, flexible polyions such as PSS may undergo local collapse in the presence of divalent ions. The mechanism of this collapse is not understood. One possibility is that condensed divalent ions neutralise two neighbouring ionic groups along the chain, which may induce local coiling beyond that expected from the reduction in the effective charge density. A decrease in the effective contour length of the chain would reduce the separation between charged groups and therefore promote additional condensation. For semiflexible chains, such an effect may be absent because the intrinsic rigidity of the backbone prevents large changes in the local conformation.

Alternatively, one could conclude that Oosawa–Manning

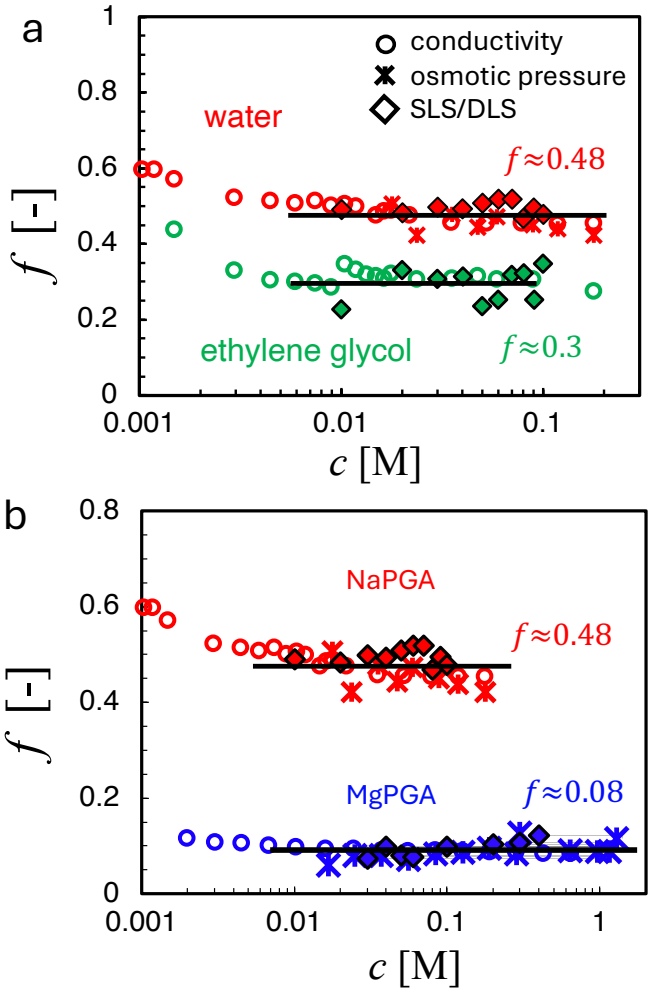

FIG. 9. Fraction of free counterions as a function of concentration for (a) NaPGA in water and EG and (b) NaPGA and MgPGA and water.

condensation does not apply and that the effective charge of polyelectrolyte chains is not inversely proportional to the counterion valence. However, this interpretation raises the question of why the predicted inverse dependence is nevertheless observed in many semiflexible polysaccharide systems.

V. CONCLUSIONS

Salt-free polyelectrolyte solutions display a long-standing inconsistency between their thermodynamic and scattering behaviour. Their large osmotic pressure implies a very low osmotic compressibility and therefore weak low-q scattering, yet experiments typically report a pronounced low-q upturn and a corresponding slow mode in dynamic light scattering.

In this work we show that these contributions can largely be removed by filtration through sufficiently small pore sizes and that the remaining signal can be separated into fast and slow components using dynamic light scattering. The static intensity of the fast component corresponds to the osmotic compressibility expected for salt-free polyelectrolyte solutions and can therefore be used to determine the fraction of free counterions. This procedure provides a practical way to obtain osmotic information from scattering measurements, which is particularly useful in non-aqueous solvents where conventional osmometric techniques are difficult to apply.

The validity of the method was demonstrated for several systems. For TBACMC and NaCMC in water, the fraction of free counterions obtained from SLS/DLS agrees well with independent estimates from electrical conductivity. For NaPGA in water, the values obtained from scattering, conductivity and freezing point depression osmometry are mutually consistent. The method also allows the effective charge of polyelectrolytes to be evaluated in non-aqueous solvents, as demonstrated for NaPGA in ethylene glycol.

Comparison of NaPGA and MgPGA shows that the divalent counterion produces a much lower fraction of dissociated counterions. This decrease is considerably stronger than predicted by the Oosawa–Manning model and contrasts with the behaviour of semiflexible polysaccharides such as CMC or alginate, where the expected inverse dependence on counterion valence is observed. One possible explanation is that flexible polyelectrolytes undergo local conformational changes in the presence of multivalent ions, effectively reducing the contour length and promoting additional condensation. Further work will be required to clarify the mechanism responsible for this behaviour.

Overall, the results show that once the contribution of the slow mode is removed, the scattering of salt-free polyelectrolyte solutions is quantitatively consistent with their thermodynamic properties. The approach presented here therefore provides a useful route to determine osmotic properties and counterion dissociation in systems where direct osmometric measurements are difficult or impossible.

ACKNOWLEDGEMENTS

SANS experiment were carried out by the JRR-3 general user program managed by the Institute for Solid State Physics, University of Tokyo (proposal ID: 24813) and at the SANS-2D beamline of the ISIS neutron source. We thank Dr. K. Mayumi and Dr. S. Rogers for their technical assistance with these experiments. We thank the SPring-8 synchrotron facility for SAXS and beamtime (proposal numbers: 2024A1203, 2025A1060 at beamline BL40B2) and Dr. Noboru Ohta and Dr. Albert Mufundirwa for their assistance with beamline setup and data reduction. We thank prof. Ralph Colby (PSU) for feedback on a draft of the manuscript.

BIBLIOGRAPHY

[1] G. S. Manning, "Limiting laws and counterion condensation in polyelectrolyte solutions i. colligative properties," J. Chem. Phys. **51**, 924–933 (1969), https://doi.org/10.1063/1.1672157.

[2] G. S. Manning, "Polyelectrolytes," Annual review of physical chemistry **23**, 117–140 (1972).

[3]F. Oosawa, *Polyelectrolytes* (Marcel Dekker, Inc. New York, 1971).

[4]A. V. Dobrynin and M. Rubinstein, "Theory of polyelectrolytes in solutions and at surfaces," Prog. Polym. Sci. **30**, 1049–1118 (2005).

[5]P.-G. De Gennes, P. Pincus, R. Velasco, and F. Brochard, "Remarks on polyelectrolyte conformation," J. Phys.-Paris **37**, 1461–1473 (1976).

[6]A. V. Dobrynin, R. H. Colby, and M. Rubinstein, "Scaling theory of polyelectrolyte solutions," Macromolecules **28**, 1859–1871 (1995).

[7]A. V. Dobrynin, "Polymer physics disentangled: An introduction for scientists and engineers," (2026).

[8]It is possible that the cross-over to $\Pi \propto c^{1.5}$ is simply due to an increase in f with concentration. Experiments show that $\xi[m] \simeq 3.3 \times 10^{-9} c^{-1/2}$, with c in mol/dm^3, corresponding to $\Pi/k_BT \simeq 50c^{1.5}$, much larger than the observed $0.35c^{1.5}$.

[9]D. Kozak, J. Kristan, and D. Dolar, "Osmotic coefficient of polyelectrolyte solutions," Zeitschrift für Physikalische Chemie **76**, 85–92 (1971).

[10]W. Essafi, F. Lafuma, D. Baigl, and C. Williams, "Anomalous counterion condensation in salt-free hydrophobic polyelectrolyte solutions: Osmotic pressure measurements," EPL **71**, 938 (2005).

[11]A. Takahashi, N. Kato, and M. Nagasawa, "The osmotic pressure of polyelectrolyte in neutral salt solutions," J. Phys. Chem. **74**, 944–946 (1970).

[12]M. Reddy and J. A. Marinsky, "Further investigation of the osmotic properties of hydrogen and sodium polystyrenesulfonates," J. Phys. Chem. **74**, 3884–3891 (1970).

[13]P. Chu and J. A. Marinsky, "Osmotic properties of poly (styrenesulfonates). i. osmotic coefficients," J. Phys. Chem. **71**, 4352–4359 (1967).

[14]N. Ise and T. Okubo, "Mean activity coefficient of polyelectrolytes. viii. osmotic and activity coefficients of poly (styrenesulfonates) of various gegenions," The Journal of Physical Chemistry **72**, 1361–1366 (1968).

[15]R. Kakehashi, H. Yamazoe, and H. Maeda, "Osmotic coefficients of vinylic polyelectrolyte solutions without added salt," Colloid Polym. Sci. **276**, 28–33 (1998).

[16]G. Boyd, "Thermodynamic properties of strong electrolyte and strong polyelectrolyte mixtures at 25 c," in *Polyelectrolytes* (Springer, 1974) pp. 135–155.

[17]O. Bonner and J. R. Overton, "The investigation of the behavior of some polysulfonates in concentrated aqueous solutions1, 2," J. Phys. Chem. **67**, 1035–1039 (1963).

[18]D. C. Boris, *Experimental studies of polyelectrolyte solution properties* (University of Rochester, 1997).

[19]B. D. Ermi and E. J. Amis, "Domain structures in low ionic strength polyelectrolyte solutions," Macromolecules **31**, 7378–7384 (1998).

[20]S. Lifson and A. Katchalsky, "The electrostatic free energy of polyelectrolyte solutions. ii. fully stretched macromolecules," Journal of Polymer Science **13**, 43–55 (1954).

[21]J. P. Donley and D. R. Heine, "Structure of strongly charged polyelectrolyte solutions," Macromolecules **39**, 8467–8472 (2006).

[22]M. Muthukumar, "Counterion adsorption theory of dilute polyelectrolyte solutions: Apparent molecular weight, second virial coefficient, and intermolecular structure factor," The Journal of Chemical Physics **137** (2012).

[23]Z. Alexandrowicz, "The correlation between activities of polyelectrolytes, measured by the light-scattering and osmotic methods," J. Polym. Sci. **40**, 91–106 (1959).

[24]S. Saha, K. Fischer, M. Muthukumar, and M. Schmidt, "Apparent molar mass of a polyelectrolyte in an organic solvent in the low ionic strength limit as revealed by light scattering," Macromolecules **46**, 8296–8303 (2013).

[25]S. Saha, *Determination of effective charge of flexible Polyelectrolytes by Light Scattering*, Ph.D. thesis, Mainz, Univ., Diss. (2013).

[26]M. Nierlich, F. Boue, A. Lapp, and R. Oberthür, "Characteristic lengths and the structure of salt free polyelectrolyte solutions. a small angle neutron scattering study," Colloid Polym. Sci. **263**, 955–964 (1985).

[27]K. Kaji, H. Urakawa, T. Kanaya, and R. Kitamaru, "Phase diagram of polyelectrolyte solutions," J. Phys. **49**, 993–1000 (1988).

[28]K. Nishida, K. Kaji, and T. Kanaya, "Charge density dependence of correlation length due to electrostatic repulsion in polyelectrolyte solutions," Macromolecules **28**, 2472–2475 (1995).

[29]J. Hone, A. Howe, and T. Cosgrove, "A small-angle neutron scattering study of the structure of gelatin/polyelectrolyte complexes," Macromolecules **33**, 1206–1212 (2000).

[30]K. Nishida, K. Kaji, and T. Kanaya, "High concentration crossovers of polyelectrolyte solutions," J. Chem. Phys. **114**, 8671–8677 (2001).

[31]J. Combet, P. Lorchat, and M. Rawiso, "Salt-free aqueous solutions of polyelectrolytes: Small angle x-ray and neutron scattering characterization," Eur. Phys. J. Spec. Top. **213**, 243–265 (2012).

[32]W. Essafi, N. Haboubi, C. Williams, and F. Boué, "Weak temperature dependence of structure in hydrophobic polyelectrolyte aqueous solution (pssna): correlation between scattering and viscosity," J. Phys. Chem. B **115**, 8951–8960 (2011).

[33]C. G. Lopez, S. E. Rogers, R. H. Colby, P. Graham, and J. T. Cabral, "Structure of sodium carboxymethyl cellulose aqueous solutions: A sans and rheology study," J. Polym. Sci. B: Polym. Phys. **53**, 492–501 (2015).

[34]C. G. Lopez, R. H. Colby, and J. T. Cabral, "Electrostatic and hydrophobic interactions in nacmc aqueous solutions: Effect of degree of substitution," Macromolecules **51**, 3165–3175 (2018).

[35]G. S. Ullmann, K. Ullmann, R. M. Lindner, and G. D. Phillies, "Probe diffusion of polystyrene latex spheres in polyethylene oxide-water," The Journal of Physical Chemistry **89**, 692–700 (1985).

[36]J. Won, C. Onyenemezu, W. G. Miller, and T. P. Lodge, "Diffusion of spheres in entangled polymer solutions: a return to stokes-einstein behavior," Macromolecules **27**, 7389–7396 (1994).

[37]R. Holyst, A. Bielejewska, J. Szymański, A. Wilk, A. Patkowski, J. Gapiński, A. Żywociński, T. Kalwarczyk, E. Kalwarczyk, M. Tabaka, *et al.*, "Scaling form of viscosity at all length-scales in poly (ethylene glycol) solutions studied by fluorescence correlation spectroscopy and capillary electrophoresis," Physical Chemistry Chemical Physics **11**, 9025–9032 (2009).

[38]S. Dou, "Synthesis and characterization of ion-containing polymers," (2007).

[39]The QP2VP used by Dou has a degree of polymerisation $\simeq 4.3$ times larger than that of Ermi and Amis' sample. We divide Dou's specific viscosity by this ratio as for non-entangled solutions η_{sp} is approximately proportional to the degree of polymerisation of the chains.[73].

[40]C. G. Lopez and W. Richtering, "Influence of divalent counterions on the solution rheology and supramolecular aggregation of carboxymethyl cellulose," Cellulose **26**, 1517–1534 (2019).

[41]M. Sedlák, "What can be seen by static and dynamic light scattering in polyelectrolyte solutions and mixtures?" Langmuir **15**, 4045–4051 (1999).

[42]A. Topp, L. Belkoura, and D. Woermann, "Effect of charge density on the dynamic behavior of polyelectrolytes in aqueous solution," Macromolecules **29**, 5392–5397 (1996).

[43]M. Muthukumar, "Ordinary–extraordinary transition in dynamics of solutions of charged macromolecules," Proceedings of the National Academy of Sciences **113**, 12627–12632 (2016).

[44]M. Sedlák and E. J. Amis, "Dynamics of moderately concentrated salt-free polyelectrolyte solutions: Molecular weight dependence," The Journal of chemical physics **96**, 817–825 (1992).

[45]M. Sedlák and E. J. Amis, "Concentration and molecular weight regime diagram of salt-free polyelectrolyte solutions as studied by light scattering," J. Chem. Phys. **96**, 826–834 (1992).

[46]H. Matsuoka, Y. Ogura, and H. Yamaoka, "Effect of counterion species on the dynamics of polystyrenesulfonate in aqueous solution as studied by dynamic light scattering," The Journal of chemical physics **109**, 6125–6132 (1998).

[47]Y. Zhang, J. F. Douglas, B. D. Ermi, and E. J. Amis, "Influence of counterion valency on the scattering properties of highly charged polyelectrolyte solutions," J. Chem. Phys. **114**, 3299–3313 (2001).

[48]A. Topp, L. Belkoura, and D. Woermann, "Dynamic light scattering experiments with aqueous solutions of polyelectrolytes of low charge density along the polymer chain in the presence of salt," Berichte der Bunsengesellschaft für physikalische Chemie **99**, 730–735 (1995).

[49]M. Sedlák, Č. Koňák, P. Štěpánek, and J. Jakeš, "Semidilute solutions of poly (methacrylic acid) in the absence of salt: Dynamic light-scattering study," Polymer **28**, 873–880 (1987).

[50]M. Drifford and J. P. Dalbiez, "Light scattering by dilute solutions of salt-free polyelectrolytes," J. Phys. Chem. **88**, 5368–5375 (1984).

[51]E. J. Amis, D. E. Valachovic, and M. Sedlák, "Structure and dynamics of linear flexible polyelectrolytes in salt-free solution as seen by light scattering," (ACS Publications, 1994).

[52]K. S. Schmitz, "On the "filterable aggregates and other particles" interpretation of the extraordinary regime of polyelectrolytes," Biopolymers: Original Research on Biomolecules **33**, 953–959 (1993).
[53]C. G. Lopez, A. Matsumoto, and A. Q. Shen, "Dilute polyelectrolyte solutions: recent progress and open questions," Soft Matter **20**, 2635–2687 (2024).
[54]M. Sedlak, "On the" filterable aggregates and other particles" interpretation of the slow polyelectrolyte mode," Macromolecules **28**, 793–794 (1995).
[55]B. D. Ermi and E. J. Amis, "Model solutions for studies of salt-free polyelectrolytes," Macromolecules **29**, 2701–2703 (1996).
[56]J. Tanahatoe and M. Kuil, "Polyelectrolyte aggregates in solutions of sodium poly (styrenesulfonate)," The Journal of Physical Chemistry B **101**, 5905–5908 (1997).
[57]B. D. Ermi and E. J. Amis, "Influence of backbone solvation on small angle neutron scattering from polyelectrolyte solutions," Macromolecules **30**, 6937–6942 (1997).
[58]H. Matsuoka and N. Ise, "Small-angle and ultra-small-angle scattering study of the ordered structure in polyelectrolyte solutions and colloidal dispersions," in *Polymer Analysis and Characterization* (Springer, 2005) pp. 187–231.
[59]R. Cong, E. Temyanko, P. S. Russo, N. Edwin, and R. M. Uppu, "Dynamics of poly (styrenesulfonate) sodium salt in aqueous solution," Macromolecules **39**, 731–739 (2006).
[60]J. F. Douglas, F. Horkay, and Y. Zhang, "Influence of counterion valency on the scattering properties of highly charged polyelectrolyte solutions revisited," The Journal of Chemical Physics **163** (2025).
[61]R. C. Michel and W. F. Reed, "New evidence of the nonequilibrium nature of the "slow modes" of diffusion in polyelectrolyte solutions," Biopolymers: Original Research on Biomolecules **53**, 19–39 (2000).
[62]S. Ghosh, R. M. Peitzsch, and W. F. Reed, "Aggregates and other particles as the origin of the "extraordinary" diffusional phase in polyelectrolyte solutions," Biopolymers: Original Research on Biomolecules **32**, 1105–1122 (1992).
[63]R. M. Peitzsch, M. J. Burt, and W. F. Reed, "Evidence of partial draining for linear polyelectrolytes; heparin, chondroitin 6-sulfate, and poly (styrene sulfonate)," Macromolecules **25**, 806–815 (1992).
[64]M. Sedlák, "Mechanical properties and stability of multimacroion domains in polyelectrolyte solutions," J. Chem. Phys. **116**, 5236–5245 (2002).
[65]M. Sedlák, "Long-time stability of multimacroion domains in polyelectrolyte solutions," J. Chem. Phys. **116**, 5246–5255 (2002).
[66]M. Sedlák, "Generation of multimacroion domains in polyelectrolyte solutions by change of ionic strength or p h (macroion charge)," The Journal of chemical physics **116**, 5256–5262 (2002).
[67]M. Sedlák, "Real-time monitoring of the origination of multimacroion domains in a polyelectrolyte solution," The Journal of chemical physics **122** (2005).
[68]G. Xu, S. Luo, Q. Yang, J. Yang, and J. Zhao, "Single chains of strong polyelectrolytes in aqueous solutions at extreme dilution: Conformation and counterion distribution," The Journal of chemical physics **145** (2016).
[69]H. Landfield, N. Kalamaris, and M. Wang, "Extreme dependence of dynamics on concentration in highly crowded polyelectrolyte solutions," Science Advances **10**, eado4976 (2024).
[70]G. Xu, J. Yang, and J. Zhao, "Molecular weight dependence of chain conformation of strong polyelectrolytes," The Journal of chemical physics **149** (2018).
[71]M. Oostwal, M. Blees, J. De Bleijser, and J. Leyte, "Chain self-diffusion in aqueous salt-free solutions of sodium poly (styrenesulfonate)," Macromolecules **26**, 7300–7308 (1993).
[72]C. G. Lopez, J. Linders, C. Mayer, and W. Richtering, "Diffusion and viscosity of unentangled polyelectrolytes," Macromolecules **54**, 8088–8103 (2021).
[73]A. Han, V. V. S. Uppala, D. Parisi, C. George, B. J. Dixon, C. D. Ayala, X. Li, L. A. Madsen, and R. H. Colby, "Determining the molecular weight of polyelectrolytes using the rouse scaling theory for salt-free semidilute unentangled solutions," Macromolecules **55**, 7148–7160 (2022).
[74]M. Sedlak, "Resolving the mystery of the extraordinary polyelectrolyte behavior (anomalously slow diffusive mode) after half-century of research," Macromolecules **58**, 5329–5343 (2025).
[75]A. Yethiraj, "Conformational properties and static structure factor of polyelectrolyte solutions," Physical review letters **78**, 3789 (1997).
[76]J.-M. Y. Carrillo and A. V. Dobrynin, "Polyelectrolytes in salt solutions: Molecular dynamics simulations," Macromolecules **44**, 5798–5816 (2011).
[77]J.-M. Carrillo, Y. Wang, R. Kumar, and B. G. Sumpter, "Coarse-grained explicit-solvent molecular dynamics simulations of semidilute unentangled polyelectrolyte solutions," The European Physical Journal E **46**, 92 (2023).
[78]L. Nová, M. Stepanek, I. Morozova, Z. Tosner, and F. Uhlík, "Ionization and chain size of weak polyelectrolytes in semidilute regime," Macromolecules **58**, 9962–9971 (2025).
[79]A. Chremos and J. F. Douglas, "Communication: Counter-ion solvation and anomalous low-angle scattering in salt-free polyelectrolyte solutions," J. Chem. Phys. **147**, 241103 (2017).
[80]M. Andreev, A. Chremos, J. de Pablo, and J. F. Douglas, "Coarse-grained model of the dynamics of electrolyte solutions," The Journal of Physical Chemistry B **121**, 8195–8202 (2017).
[81]A. Chremos and J. F. Douglas, "The influence of polymer and ion solvation on the conformational properties of flexible polyelectrolytes," Gels **4**, 20 (2018).
[82]A. Chremos and J. F. Douglas, "Polyelectrolyte association and solvation," J. Chem. Phys. **149**, 163305 (2018).
[83]D. L. Ho, B. Hammouda, and S. R. Kline, "Clustering of poly (ethylene oxide) in water revisited," Journal of Polymer Science Part B: Polymer Physics **41**, 135–138 (2003).
[84]B. Hammouda, D. L. Ho, and S. Kline, "Insight into clustering in poly (ethylene oxide) solutions," Macromolecules **37**, 6932–6937 (2004).
[85]F. Horkay and B. Hammouda, "Small-angle neutron scattering from typical synthetic and biopolymer solutions," Colloid and Polymer Science **286**, 611–620 (2008).
[86]B. Hammouda, "The mystery of clustering in macromolecular media," Polymer **50**, 5293–5297 (2009).
[87]B. Hammouda, "Clustering in polar media," The Journal of chemical physics **133** (2010).
[88]B. Hammouda, F. Horkay, and M. L. Becker, "Clustering and solvation in poly (acrylic acid) polyelectrolyte solutions," Macromolecules **38**, 2019–2021 (2005).
[89]J. S. Higgins and H. C. Benoit, "Polymers and neutron scattering," (1994).
[90]The main type of commercially available osmometers today are based on freezing point depression. These instruments are designed for aqueous solutions and are unlikely to be adapted to organic solvents because measuring the freezing point of many organics is difficult due to their low melting temperatures. The few available vapour pressure and membrane osmometers (e.g. BMT 923, Vapro-5600) are also designed primarily for aqueous solutions.
[91]C. G. Lopez, "Entanglement of semiflexible polyelectrolytes: Crossover concentrations and entanglement density of sodium carboxymethyl cellulose," J. Rheol. **64**, 191–204 (2020).
[92]A. Gulati, J. F. Douglas, O. Matsarskaia, and C. G. Lopez, "Influence of counterion type on the scattering of a semiflexible polyelectrolyte," Soft matter **20**, 8610–8620 (2024).
[93]A. Gulati, L. Meng, C. Hou, T. Watanabe, and C. G. Lopez, "Solution structure and counterion condensation of carboxymethyl cellulose in organic solvents." Submitted to ACS Applied Polymer Materials (2026).
[94]H. Wu, "Correlations between the rayleigh ratio and the wavelength for toluene and benzene," Chemical Physics **367**, 44–47 (2010).
[95]T. E. Sweeney and C. A. Beuchat, "Limitations of methods of osmometry: measuring the osmolality of biological fluids," American Journal of Physiology-Regulatory, Integrative and Comparative Physiology (1993).
[96]R. H. Colby, "Structure and linear viscoelasticity of flexible polymer solutions: comparison of polyelectrolyte and neutral polymer solutions," Rheol. Acta **49**, 425–442 (2010).
[97]C. G. Lopez, "Scaling and entanglement properties of neutral and sulfonated polystyrene," Macromolecules **52**, 9409–9415 (2019).
[98]Note that the choice of monomer (e.g., chemical vs. Kuhn monomer) is not important because the product *bc* does not change.
[99]Note that this definition, following ref. [6] is different from that in refs. [132,133].

[100]K. Salamon, D. Aumiler, G. Pabst, and T. Vuletic, "Probing the mesh formed by the semirigid polyelectrolytes," Macromolecules **46**, 1107–1118 (2013).
[101]E. A. GharehTapeh, T. Watanabe, F. Horkay, C. Hou, C. Lopez, and M. Hohenschutz, "Counterion condensation, ion pairing and scattering properties of carboxymethyl cellulose with mono- and divalent ions." Cellulose, accepted (2026).
[102]E. Di Cola, N. Plucktaveesak, T. Waigh, R. Colby, J. Tan, W. Pyckhout-Hintzen, and R. Heenan, "Structure and dynamics in aqueous solutions of amphiphilic sodium maleate-containing alternating copolymers," Macromolecules **37**, 8457–8465 (2004).
[103]S. Dou and R. H. Colby, "Solution rheology of a strongly charged polyelectrolyte in good solvent," Macromolecules **41**, 6505–6510 (2008).
[104]C. G. Lopez, F. Horkay, R. Schweins, and W. Richtering, "Solution properties of polyelectrolytes with divalent counterions," Macromolecules **54**, 10583–10593 (2021).
[105]F. Oosawa, "A simple theory of thermodynamic properties of polyelectrolyte solutions," J. Polym. Sci. **23**, 421–430 (1957), https://onlinelibrary.wiley.com/doi/pdf/10.1002/pol.1957.1202310335.
[106]G. S. Manning, "The molecular theory of polyelectrolyte solutions with applications to the electrostatic properties of polynucleotides," Quarterly reviews of biophysics **11**, 179–246 (1978).
[107]M. Beer, M. Schmidt, and M. Muthukumar, "The electrostatic expansion of linear polyelectrolytes: Effects of gegenions, co-ions, and hydrophobicity," Macromolecules **30**, 8375–8385 (1997).
[108]A. Matsumoto, R. Ukai, H. Osada, S. Sugihara, and Y. Maeda, "Tuning the solution viscosity of ionic-liquid-based polyelectrolytes with solvent dielectric constants via the counterion condensation," Macromolecules **55**, 10600–10606 (2022), https://doi.org/10.1021/acs.macromol.2c01405.
[109]C. Wandrey, D. Hunkeler, U. Wendler, and W. Jaeger, "Counterion activity of highly charged strong polyelectrolytes," Macromolecules **33**, 7136–7143 (2000).
[110]C. Wandrey, "Concentration regimes in polyelectrolyte solutions," Langmuir **15**, 4069–4075 (1999).
[111]Q. Tang and M. Rubinstein, "Where in the world are condensed counterions?" Soft matter **18**, 1154–1173 (2022).
[112]D. Kozak, "Osmotic coefficients of maleic acid/ethylene copolymer solutions," Die Makromolekulare Chemie: Macromolecular Chemistry and Physics **177**, 287–292 (1976).
[113]W. Kern, "Über heteropolare molekülkolloide. i. die polyacrylsäure, ein modell des eiweißes 185. mitteilung über hochpolymere verbindungen," Zeitschrift für Physikalische Chemie **181**, 249–282 (1937).
[114]M. Nagy, "Thermodynamic study of aqueous solutions of polyelectrolytes of low and medium charge density without added salt by direct measurement of osmotic pressure," The Journal of Chemical Thermodynamics **42**, 387–399 (2010).
[115]M. Nagy, "Thermodynamic study of polyelectrolytes in aqueous solutions without added salts: a transition from neutral to charged macromolecules," The Journal of Physical Chemistry B **108**, 8866–8875 (2004).
[116]D. Baigl, *Etude experimentale de polyelectrolytes hydrophobes modeles*, Ph.D. thesis, Paris VI (2003).
[117]R. H. Colby, D. C. Boris, W. E. Krause, and J. S. Tan, "Polyelectrolyte conductivity," J. Polym. Sci. B: Polym. Phys. **35**, 2951–2960 (1997).
[118]F. Bordi, C. Cametti, and R. Colby, "Dielectric spectroscopy and conductivity of polyelectrolyte solutions," J. Phys. Condens. Matter **16**, R1423 (2004).
[119]Y. Marcus, "Tetraalkylammonium ions in aqueous and non-aqueous solutions," Journal of Solution Chemistry **37**, 1071–1098 (2008).
[120]J. S. Behra, J. Mattsson, O. J. Cayre, E. S. Robles, H. Tang, and T. N. Hunter, "Characterization of sodium carboxymethyl cellulose aqueous solutions to support complex product formulation: A rheology and light scattering study," ACS Appl. Polym. Mater. **1**, 344–358 (2019).
[121]W. Brown, D. Henley, and J. Ohman, "Sodium carboxymethyl cellulose experimental study of influence of molecular weight and ionic strength on polyelectrolyte configuration," Arkiv Kemi **22**, 189–206 (1964).
[122]D. Ray, R. De, and B. Das, "Thermodynamic, transport and frictional properties in semidilute aqueous sodium carboxymethylcellulose solution," J. Chem. Thermodyn. **101**, 227–235 (2016).
[123]W. N. Sharratt, R. O'Connell, S. E. Rogers, C. G. Lopez, and J. T. Cabral, "Conformation and phase behavior of sodium carboxymethyl cellulose in the presence of mono-and divalent salts," Macromolecules **53**, 1451–1463 (2020).
[124]This interpretation is supported by density experiments, which show no measurable change in solution density after filtering.
[125]Note that Manning's theory expects each counterion to contribute $\simeq 0.5$ to the osmotic pressure. Therefore, f calculated from Manning's full theory should be $\simeq 0.96$, or around 37% larger than the theoretical value.
[126]M. Jacobs, C. G. Lopez, and A. V. Dobrynin, "Quantifying the effect of multivalent ions in polyelectrolyte solutions," Macromolecules **54**, 9577–9586 (2021).
[127]M. Rinaudo and B. Loiseleur, "Propriétés des solutions aqueuses de polyélectrolytes en présence de sels neutres-ii.—propriétés thermodynamiques," Journal de Chimie Physique **70**, 1697–1701 (1973).
[128]M. Rinaudo and M. Milas, "Interaction of monovalent and divalent counterions with some carboxylic polysaccharides," J. Polym. Sci., Polym. Chem. Ed. **12**, 2073–2081 (1974).
[129]M. Rinaudo and M. Milas, "Ionic selectivity of polyelectrolytes in salt free solutions," in *Polyelectrolytes and their Applications* (Springer, 1975) pp. 31–49.
[130]C. Yomota, S. Okada, K. Mochida, and M. Nakagaki, "The molal osmotic coefficients and counterion activity coefficients of arabate with various counterions," Chemical and pharmaceutical bulletin **32**, 3793–3802 (1984).
[131]H. T. Masakatsu Yonese and H. Kishimoto, "Practical osmotic coefficients of chondroitin sulfate a and c salts with various counterions," Journal of the Chemical Society of Japan (Chemistry and Industrial Chemistry) **1978**, 108–112 (1978).
[132]A. V. Dobrynin and M. Jacobs, "When do polyelectrolytes entangle?" Macromolecules **54**, 1859–1869 (2021).
[133]A. V. Dobrynin, M. Jacobs, and R. Sayko, "Scaling of polymer solutions as a quantitative tool," Macromolecules **54**, 2288–2295 (2021).